ИНСТИТУТ ЯДЕРНОЙ ФИЗИКИ СО АН СССР

V.A. Alexandrov, A.A. Mikhailichenko

METHOD OF THE MAGNETIC MEASUREMENT WITH THE CONSIDERATION OF THE FRINGE FIELD

PREPRINT 91-69

НОВОСИБИРСК

Method of the magnetic measurement with the consideration of the fringe field.

Alexandrov V.A., Mikhailichenko A.A.

Branch of the Institute of Nuclear Physics (INP)
Siberian Division of Academy of Science
142284 Moscow region, Protvino

Abstract.

In this work description of the construction and main principles of the work of the measurer of magnetic field is presented. Method of measurement is based on the spectrum analysis of the signal from rotation induction coils.

Measurer has sensitivity for the field harmonics on the level of 4 10^{-4} from the main harmonic about 5 kG/cm on the radius = 0.8 cm.

The measurer was used for testing of the elements of magnet structure of the FFTB Project (SLAC, USA).

1. Introduction.

The Final Focus Test Beam project [1] will be able to provide the beam of 50 GeV electrons with extremely small vertical size ≅ 0.06 micrometer. So, in quadrupole lenses of the FFTB maximum non-principle field at 70% of full aperture of 23 mm does not achieves 5 10^{-4} from the field of the main harmonic about 5 kG/cm.

As participants of this project, INP in Novosibirsk and its Branch in Protvino are obliged to fabricate all elements of the magnet system of FFTB. It includes 30 quadrupoles with aperture 23 mm, 4 35-mm-aperture and 6 54-mm-aperture quadrupoles, 18 dipoles and 5 sextupoles. This lead us the necessity to develop the technology of the magnetic measurements with necessary accuracy.

In this work description of the stend for magnetic measurements is presented which allows to get information about space-distribution of the field of any harmonic until 14 pole.

Stend is equipped by two power supplies (16 kW each). Operations of measurement process are full-aromatically.

2. General arrangement of the stend.

The stend consists of 3 parts: own measurer, system which provide it movement along measuring element, and electronic equipment fig.1.

Block of induction coils was used as the sensor of the magnetic field (fig.2). Each coil was wounded by the wire of 30 mkm diameter wire, has 8000 turns and placed radially to the axis of transducer's rotation.

Sensor is rotating by synchro-motor whose frequency is determined by the quartz-generator turning to the 46 Hz. By application of the rubber strap and flywheel this frequency is decreased until 8 Hz.

Sensor and so called encoder are established at the same axis. Encoder is the special block which serve for producing 32 reper points "measurement". In each of these points reading-out of the coil's signal is executed. Also encoder carry out the phasing of measurements with help of one impulse "start".

Measurer by means of linear support bearings is established at the ball bushing shaft and is able to move along the axis of the measuring magnet with help of step-motor and screw shaft. Screw shaft, ball bushing shaft and linear support bearings are extremely precision that provides accuracy of movement on the level of 50 mkm.

All of control-measurement and monitor devices are fulfilled in CAMAC standard. They consist of digital 15-bit voltmeter with 256 words-memory for the reading-out of the main signal from the sensor, digital 24-bit voltmeter for the control of the excitation current, unit for the step-motor operation, special unit for the operation of the measurement process, power supply for synchro-motor, 8-channel transcoder to operate of power supplies. By means of Camac-controller and serial interface all of devices are connected to the personal computer IBM PC AT-286.

Moreover, stend is equipped by two power supplies (16 kw each). Operation of them is independent and full-automatic. Pulsates suppression block provides stability of excitation current on the level of $5\ 10^{-4}$.

3. Method of measurement.

Method of measurements of the stationarity field is based on the spectrum analysis of the signal from rotation induction coils. On fig.3 you can see the time-diagram of the measurement process.

Measurement cycle starts when the special unit gets impulse "start". From this moment for each of 32 impulses "measurement" special unit gives permission for ADC to read signal from the system of induction coils. ADC is 15-bit digital voltmeter, which is able to remember 256 values of measuring signal with interval not less than 100 mks.

Therefore, during the 8 periods of the measurement cycle we get 256 values of the signal. They determine configuration of the magnetic field, where induction coils are rotated. With help of Fourier transform we can to get information about spectrum structure of this field i.e. to determine the amplitude and phase of the first harmonic (dipole), 2-nd (quadrupole), third (sextupole) and so on.

We must to underline that from this harmonics only each 8-th is physical, and others characterize noise. This connected with Fourier transform on 8 periods of coils rotations.

After this analysis all system by means of step motor and screw shaft is moved along the axis of measuring magnet on the definite distance and process is repeated.

In each point result of measurement is output as the table of amplitudes and phases of harmonics.

If we have such information, we can to plot s-axis-distribu-

tion of any field's harmonic. However, this distribution demand the right interpretation with taken into account of the definite length of the coil and specific field at the border of the element.

4. Signal from coils (s-axis distribution).

As it can pointed out [3], the voltage from the 1-turn coil can be represented

$$U(s,t)=\sum_{m=1} U_m(s,t)=-2\Delta \sum_{m=1} r_0^m \sin(m\chi_0)\cos(m\int\omega(t)dt)\left[\overline{G_{m-1}} - \frac{(m+2)\,r^2}{4m\,(m+1)}\overline{\frac{d^2G_{m-1}}{ds^2}}+\dots\right]$$

where χ_0 - half-angular size of the coil

$$\overline{G_{m-1}}(s)=\frac{1}{\Delta}\int_{s}^{s+\Delta} G_{m-1}(\zeta)\,d\zeta$$

Let's introduce signification $U_m=U_{m_0}\cos(m\int\omega(t)dt)$:

$$U_{m_0}(s)=K_m\left[\overline{G_{m-1}}(s) - L_{m_1}\overline{\frac{d^2G_{m-1}}{ds^2}} + L_{m_2}\overline{\frac{d^4G_{m-1}}{ds^4}} - \dots\right]$$

where $K_m=-2\Delta\, r_0^m \sin(m\chi_0)$, $L_{m_1}=\frac{(m+2)}{4m\,(+1)}r_0^2$, $L_{m_2}=\frac{(m+4)r^2}{32m\,(m+1)(m+2)},\dots$

Coefficients K_m are finded from the coil's calibration at field with definite spectrum structure.

As stated above, coil gets us average value of G_{m-1} and $d^{2k}G_{m-1}/ds^{2k}$, $(k = 1,2,\dots)$ along the coil.

$$U_m(s)=K_m\frac{1}{\Delta}\int_{s}^{s+\Delta}\left[G_{m-1}(\zeta) - L_{m_1}\frac{d^2G_{m-1}}{d\zeta^2} + L_{m_2}\frac{d^4G_{m-1}}{d\zeta^4} - \dots\right]d\zeta=$$

Let's introduce indefinite limit of integration by means of difference core : $U_m(s) = K_m\frac{1}{\Delta}\int_{-\infty}^{+\infty} K(s,\zeta,\Delta)\,Q_{m-1}(\zeta)\,d\zeta$

where $K(s,\zeta,\Delta)=\begin{cases}1, & |s-\zeta| \le \frac{\Delta}{2}\\ 0, & |s-\zeta| > \frac{\Delta}{2}\end{cases}$, and

$$Q_{m-1}(s)=G_{m-1}(s) - L_{m_1}\frac{d^2G_{m-1}}{ds^2} + L_{m_2}\frac{d^4G_{m-1}}{ds^4} - \dots$$

By transforming from the $Q_{m-1}(\zeta)$ to it Fourier-image $Q_{m-1}(p)$, have:

$$U_m(s)=K_m\frac{1}{2\pi i\Delta}\int_{-\infty}^{+\infty}\frac{2}{p}e^{ps}\sin(\frac{\Delta}{2}p)\,Q_{m-1}(p)\,dp\ ;$$

By comparing of this expression with the Fourier transform of the

function $U_m(s)=\frac{1}{2\pi i}\int U_m(p)\, e^{ps} dp$, we have finally

$$G_{m-1}(p)= \frac{p\Delta}{2K_m} \frac{1}{\sin(\frac{\Delta p}{2})} \frac{1}{1-L_{m_1} p^2+L_{m_2} p^4} U_m(p)$$

Analogous results can be get for the coil with definit size by integration of these expresions for diferent r and Δ.

All of these procedures are realized by means of program and may be taken into account under consider of the measurement results. At the fig.4 s-distribution of the gradient of field of the standard quadrupole lens without consideration of derivation (curve 1) and with consideration of $d^{2k}G_{m-1}/ds^{2k}$ (curve 2).

At this figure you can see, that consideration of derivation $d^{2k}G_{m-1}/ds^{2k}$ leads to filleting of this distribution at the border of magnet.

However, even derivations we must to take into account *once more* during the restarting of picture of the field under definite values of multipole on the axis.

For the field of dipole [3]:

$$\begin{cases} B_x(x,y,s)= 2(S - \frac{1}{8}\cdot B''(s))\cdot xy + \dots \\ B_y(x,y,s)=B + (S - \frac{1}{8}\cdot B''(s))\cdot x^2 - (S + \frac{3}{8}\cdot B''(s))\cdot y^2 + \dots \end{cases}$$

So, measurement of the ideal dipole must to show the presence of the sextupole component of the field at it border : $S(s) = \frac{1}{8}\cdot B''(s)$

All of these reasoning are well illustrated by results of measurements. Fig.5 shows s-distribution of measured sextupole component of the field at the border of the dipole magnet (line 1), $\frac{1}{8}\cdot B''(s)$ (line 2) and their sum, i.e. result sextupole for decomposition of the field by means of degrees of x with y=0 (line 3). You can see, that result sextupole practically equal to zero, how probably at the sufficiently "flat" dipole magnet.

Analogously can be proved that measurement of the ideal quadrupole must to show the presence of the octupole component of the field at it border : $O(s) = \frac{1}{12} G''(s)$

and dodecapole : $D(s) = \frac{1}{384} G^{IV}(s)$

5. Results of measurements.

In conclusion we would like to present some typical results of measurement, which was made at this stend. First of all, this is s-distribution of any field-harmonic till to 14-pole. During the output phase of the harmonic is taken into account and each proection of it are plotted separately. That gives us the information about the space-position of this harmonic. The origin of excesses at the fringe of the element was discussed in the forth part of this work.

If we have information about spectrum structure of the field

of the measuring magnet, we can to plot the dependence of integral of any harmonic verse transverse radius (fig.6). Plot shows, that till $r_z \cong 0.4$ cm integral decreases linearly, how should be in the field of the quadrupole with sextupole component, and than it decreases stronger by result of influence of higher harmonics. Under $r \cong 0.8$ cm (70% of aperture) difference achieves relative value of $2.41\ 10^{-4}$.

6. Acknowledgement.

The authors wish to thank V.E.Balakin for support this work and A.V.Chernyshov for the help during the preparation and providing of measurements.

7. References.

1. Final Focus Test Beam. Project design report. Sept. 1990, SLAC, Stanford, California.
2. CERN Courier, N3, p.10, 1991.
3. Mikhailichenko A.A., The Fringe Fields, Preprint INP 79-98, 1979.

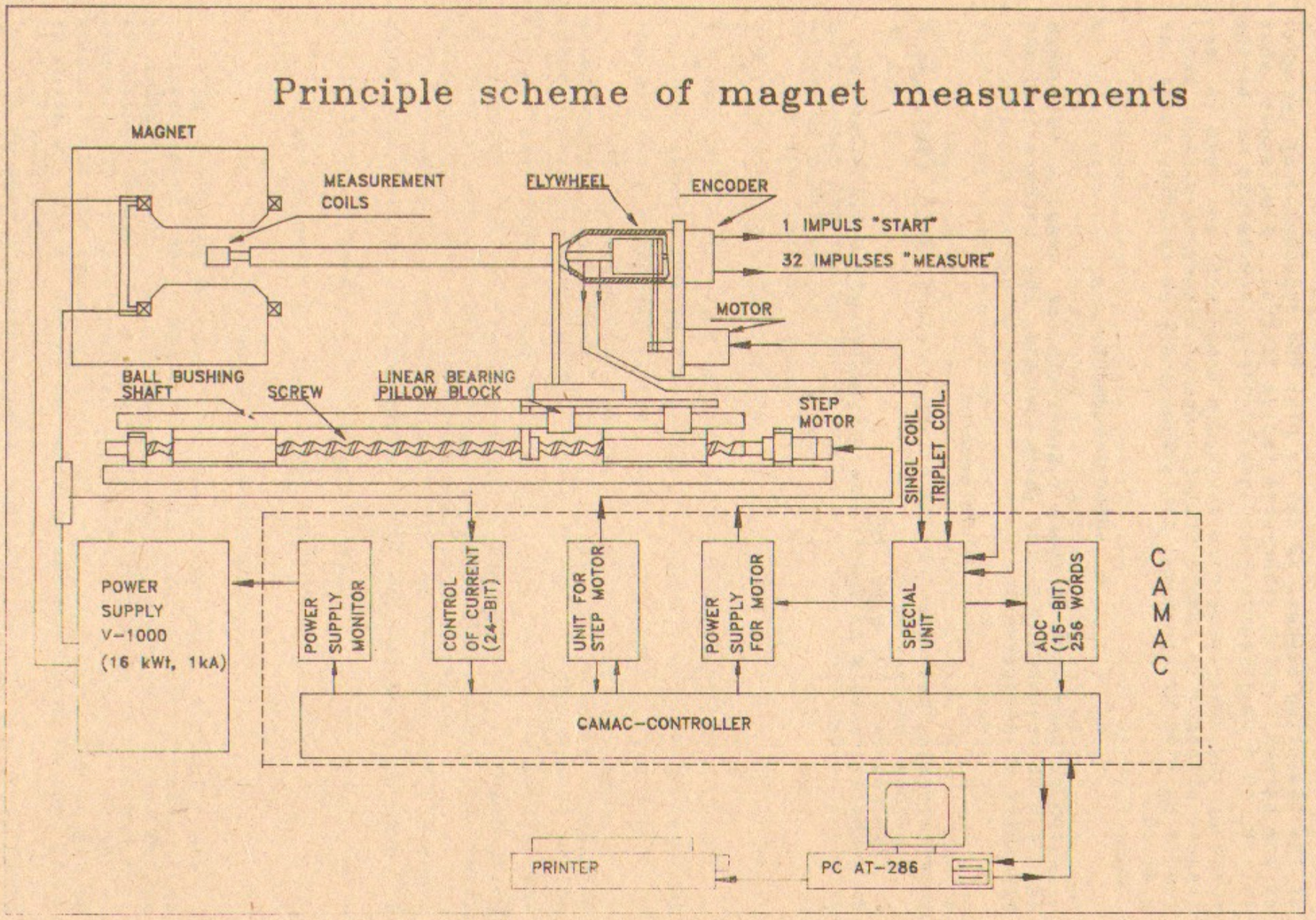

Fig.1 Equipment of the stend.

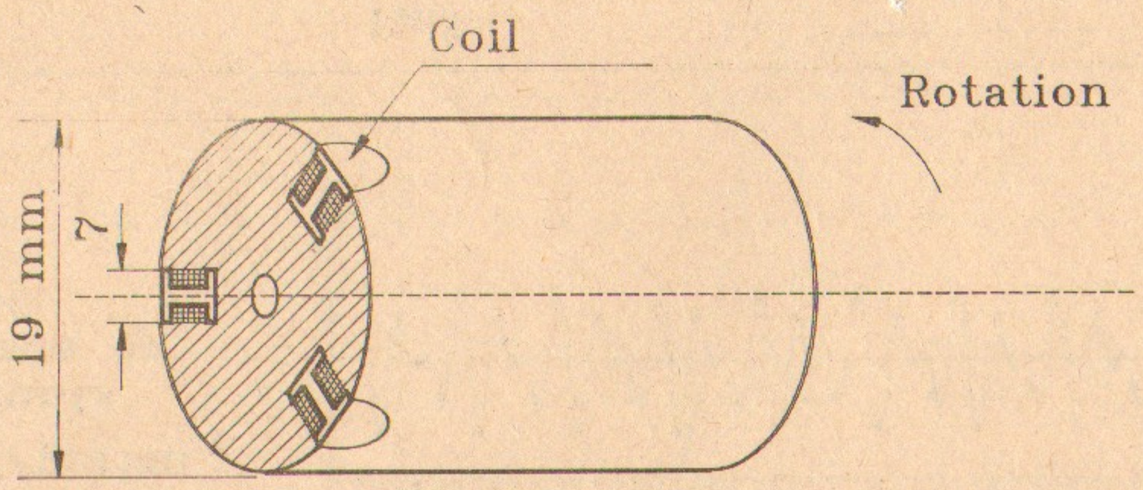

Fig. 2
Coils. It is possible to take signal from one of the coil or from all of coils.

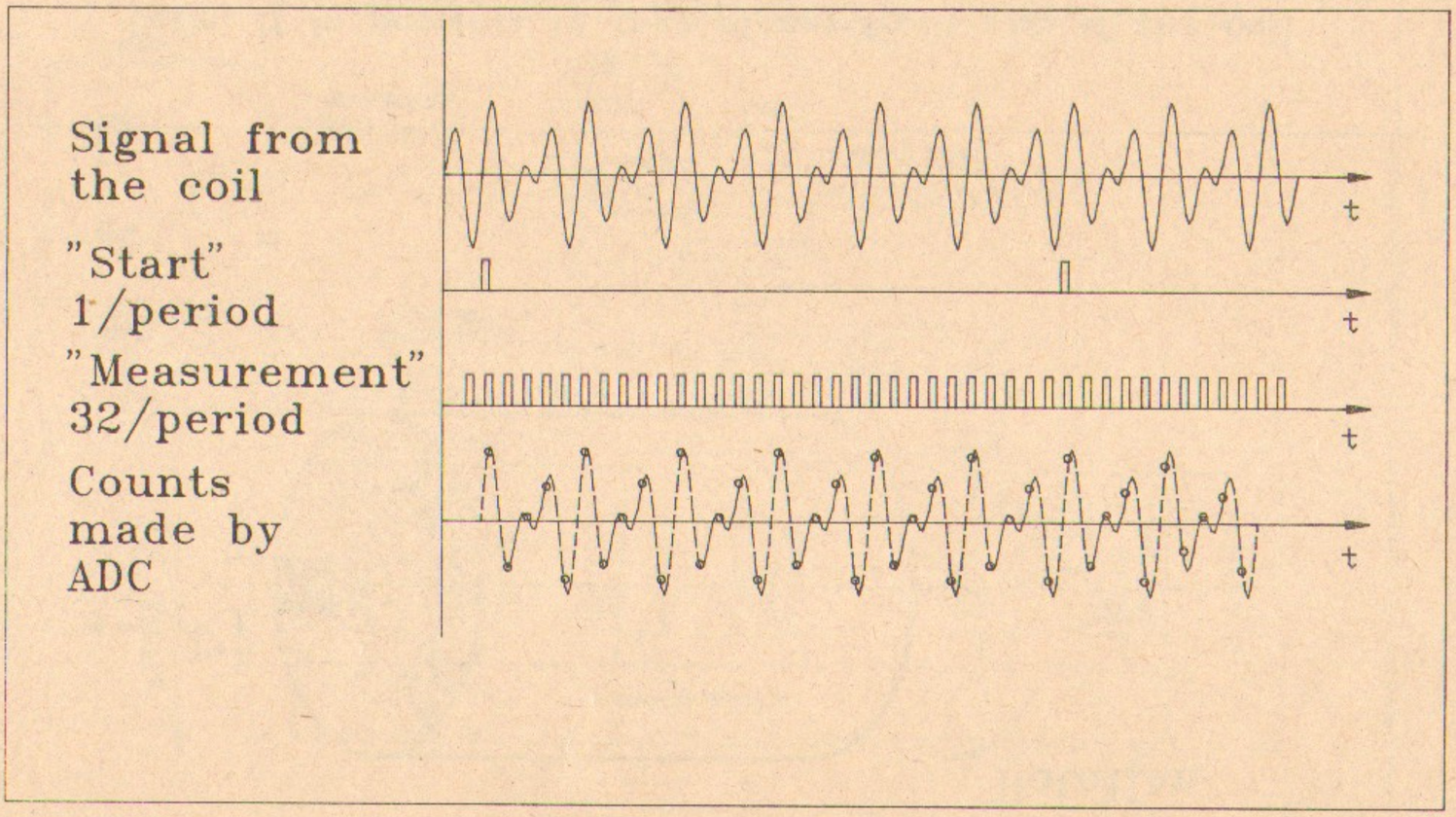

Fig.3

Time-diagram of the process of measuring.

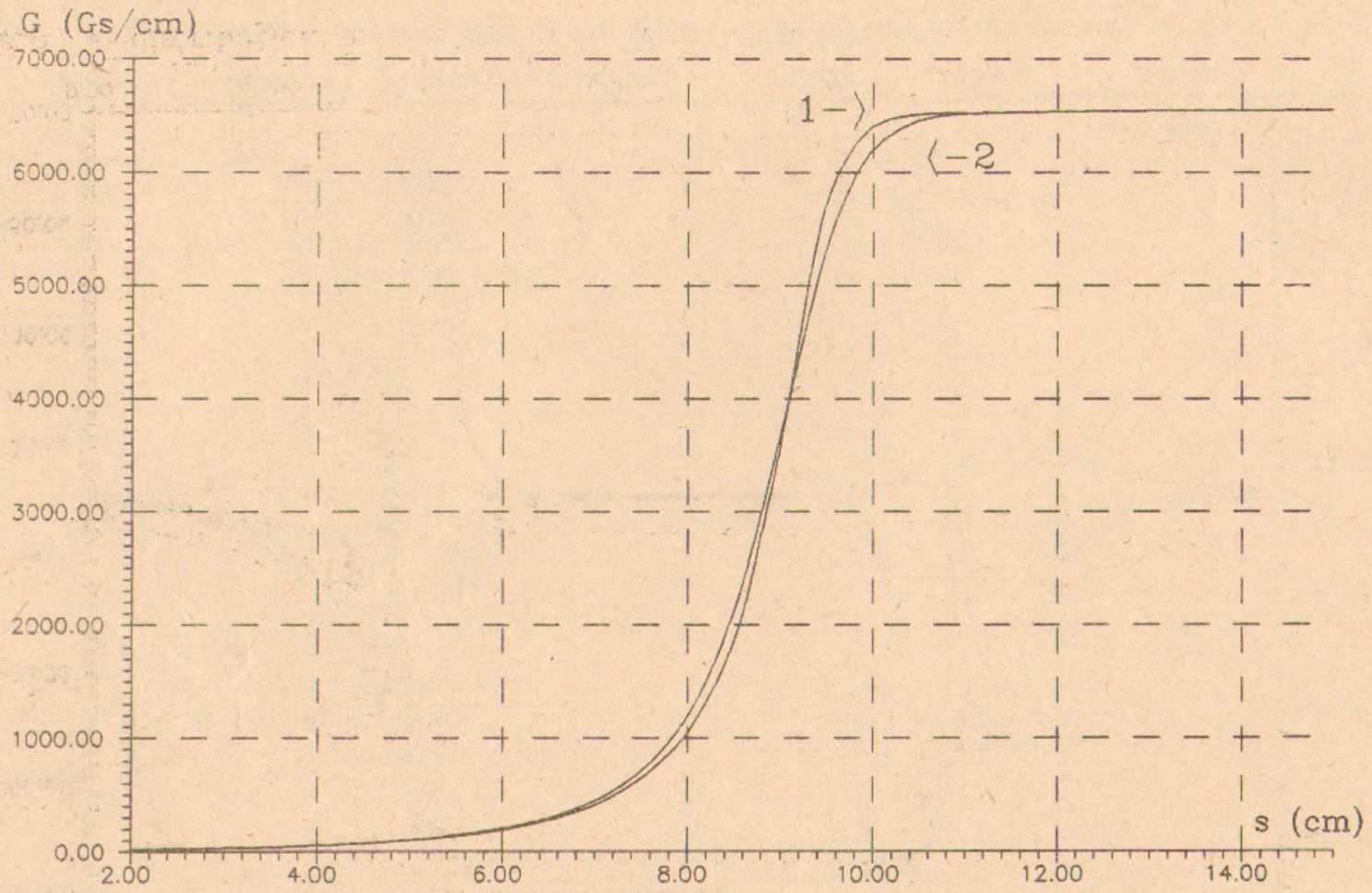

Fig. 4 s-distribution of the gradient at the border of quadrupole.

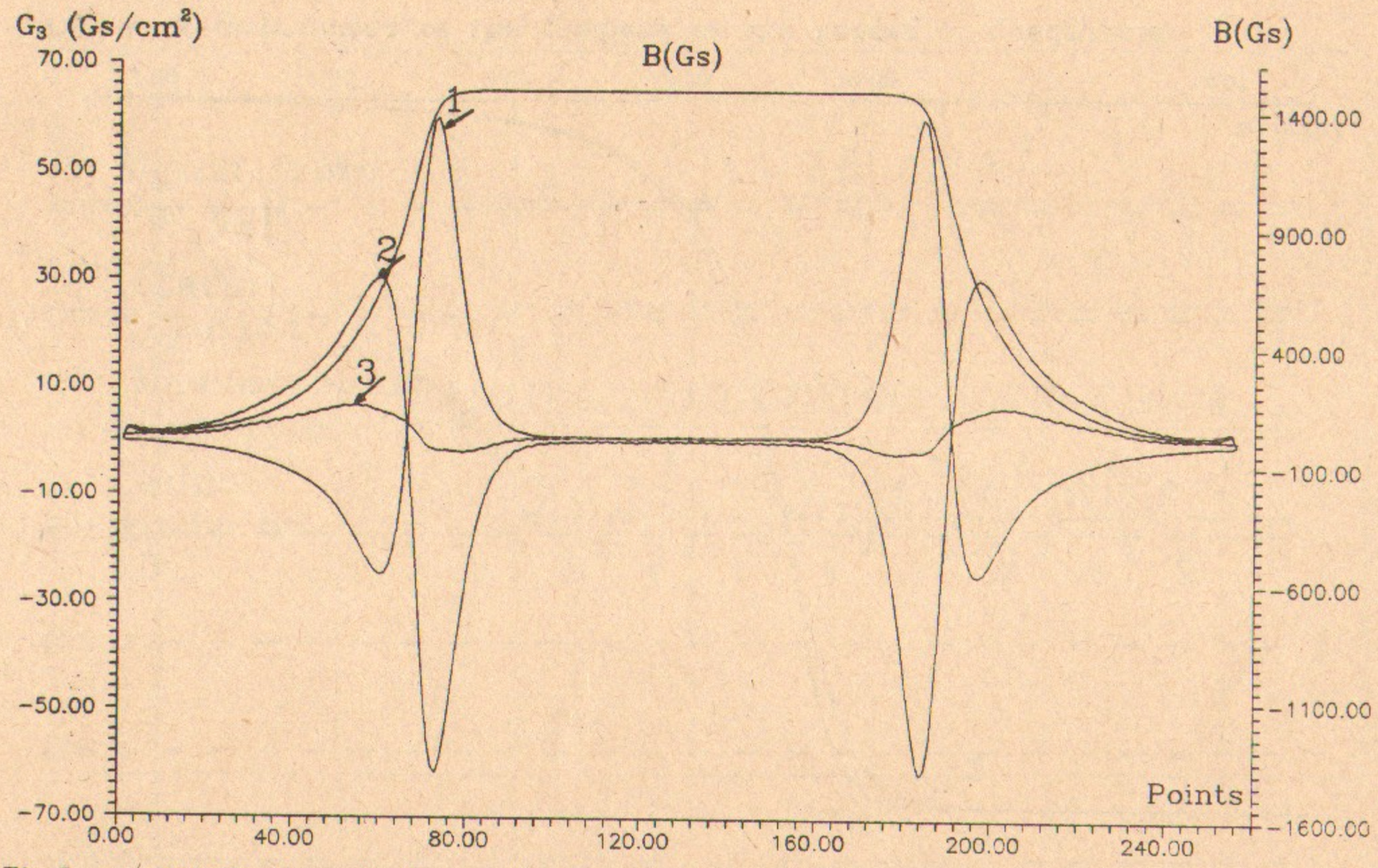

Fig.5 s-distribution of the sextupole field at the border of dipole.

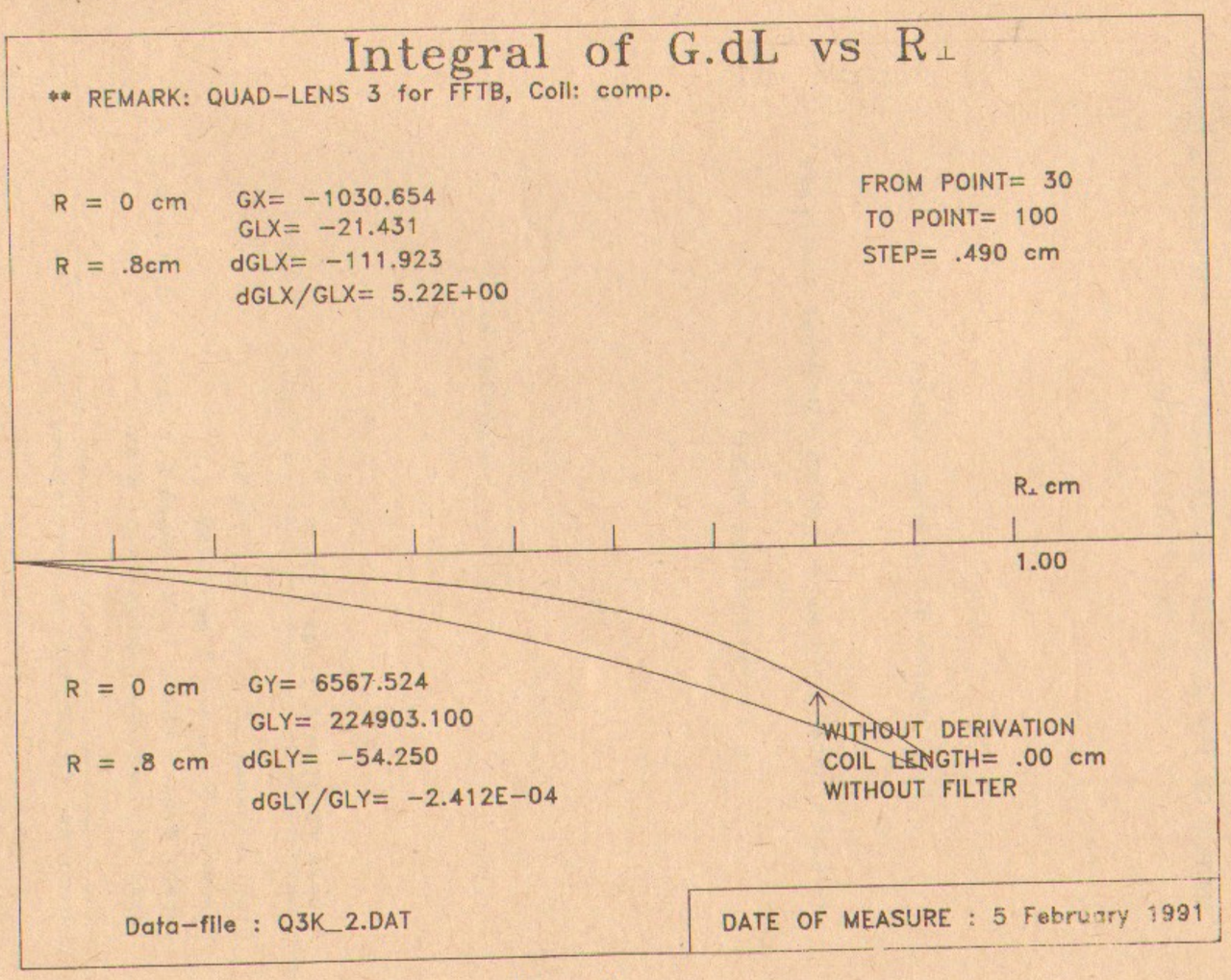

Fig. 6
Integral of G.dL vs R⊥.

Alexandrov V.A., Mikhailichenko A.A.

METHOD OF THE MAGNETIC MEASUREMENT WITH THE CONSIDERATION OF THE FRINGE FIELD

Александров В.А., Михайличенко А.А.

МЕТОДИКА ПРОВЕДЕНИЯ ВЫСОКОТОЧНЫХ МАГНИТНЫХ ИЗМЕРЕНИЙ С УЧЕТОМ КРАЕВЫХ ПОЛЕЙ

ПРЕПРИНТ 91-69

Работа поступила 7 мая 1991 г.

Ответственный за выпуск С.Г.ПОПОВ
Подписано к печати 9 июля 1991 г.
Формат бумаги 60x90 1/16, Объем 0,9 печ.л., 0,8 уч.изд.л.
Тираж 180 экз. Бесплатно Заказ № 69

Ротапринт ИЯФ СО АН СССР, г.Новосибирск, 90